Materials and Manufacturing Processes, 22: 659–667, 2007

ISSN: 1042-6914 print/1532-2475 online
DOI: 10.1080/10426910701323631

Identification of Constitutive Material Model Parameters for High-Strain Rate Metal Cutting Conditions Using Evolutionary Computational Algorithms

Tuğrul Özel and Yiğit Karpat

Department of Industrial and Systems Engineering, Rutgers University, Piscataway, New Jersey, USA

Advances in plasticity-based analytical modeling and finite element methods (FEM) based numerical modeling of metal cutting have resulted in capabilities of predicting the physical phenomena in metal cutting such as forces, temperatures, and stresses generated. However, accuracy and reliability of these predictions rely on a work material constitutive model describing the flow stress, at which work material starts to plastically deform. This paper presents a methodology to determine deformation behavior of work materials in high-strain rate metal cutting conditions and utilizes evolutionary computational methods in identifying constitutive model parameters. The Johnson–Cook (JC) constitutive model and cooperative particle swarm optimization (CPSO) method are combined to investigate the effects of high-strain rate dependency, thermal softening and strain rate-temperature coupling on the material flow stress. The methodology is applied in predicting JC constitutive model parameters, and the results are compared with the other solutions. Evolutionary computational algorithms have outperformed the classical data fitting solutions. This methodology can also be extended to other constitutive material models.

Keywords Constitutive material models; High-strain rate plasticity; Metal cutting; Particle swarm optimization.

1. Introduction

The modeling and simulation of metal cutting have become very important in order to decrease the cost of experimental investigations. Continuum mechanics based finite element methods (FEM) and plasticity based analytical modeling are used in predicting the mechanics of cutting such as forces, temperatures, and stresses. These methods utilize and rely on work material constitutive models to simulate deformation conditions take place in metal cutting. Therefore, identification of constitutive material model parameters considering high-strain rate deformation characteristics is crucial. The flow stress, $\bar{\sigma}$, depends on effective strain, $\bar{\varepsilon}$, strain rate, $\dot{\bar{\varepsilon}}$, and temperature, T, of the high strain rate deformations exerted in the cutting zone. For low to moderate strain rates, the flow stress data can be obtained through compression and Split Hopkinson Pressure Bar (SHPB) tests at elevated temperature levels. However, those are not sufficient to model high-strain rate deformation behavior in high-speed metal cutting, in which extremely high and localized strains, strain rates, and temperatures are encountered [1–4]. For instance, while the strain rates around $10^5\,\mathrm{s}^{-1}$ can be obtained by SHPB compression tests, average strain rates around $20{,}000\,\mathrm{s}^{-1}$ are seen in the shearing zone during actual high-speed cutting [5]. In metal cutting, elastic strains are much lower than plastic strains hence metal mostly flows plastically into the cutting zone. Flow stress is also dependent upon other factors such as microstructures and loading histories including strain rate-temperature coupling which cannot be overlooked for microscale analysis [6–8]. The microstructure and phase transformation play a significant role on flow stress behavior during machining using small-undeformed chip loads such as in micromachining. The strain rate and temperature coupling effect is especially important for high speed cutting in which thermal softening becomes more dominant.

Consequently, accurate and reliable rate dependent constitutive models are required to represent the plasticity behavior of metals undergoing high-strain rate deformations. Accurate modeling of dynamic mechanical behavior is the prerequisite for an effective analysis for manufacturing processes. An analysis of such a complex deformation state poses great difficulties. Empirical and semiempirical constitutive models have been developed to model flow stress with certain accuracy in high-speed cutting. Most of these constitutive models are based on a range of assumptions in order to avoid the prevailing complexities in metal cutting. The success of a particular constitutive model depends on how effectively it represents physics of metal cutting as well as its ability to capture all relevant deformation parameters in a constitutive equation. In that respect, use of advanced computational methods and algorithms to determine most accurate constitutive models from the experimental data becomes highly critical and important. The objective of this work is to explore and recalculate the parameters of the constitutive models determined by using such method, cooperative particle swarm optimization, and investigate the effects of high-strain rate dependency, thermal softening, and strain rate-temperature coupling on the material flow stress.

2. Assessment of constitutive material models

To model flow stress behavior in metal cutting, several researchers have proposed specific flow stress expressions.

Received August 1, 2006; Accepted September 30, 2006
Address correspondence to Tuğrul Özel, Department of Industrial and Systems Engineering, Rutgers University, Piscataway, NJ 08854, USA; Fax: +1 732 445 5467; E-mail: ozel@rci.rutgers.edu

Oxley [1] proposed that flow stress can be expressed as a work-hardening behavior as given in Eq. (1) where σ_0 and n are written as functions of a velocity modified temperature, in which strain rate and temperature are combined into a single function as given in Eq. (2):

$$\bar{\sigma} = \sigma_0 \bar{\varepsilon}^n \tag{1}$$

$$T_{MOD} = T\left[1 - \upsilon \log\left(\frac{\dot{\bar{\varepsilon}}}{\dot{\bar{\varepsilon}}_0}\right)\right]. \tag{2}$$

where σ_0 is strength coefficient, n is strain hardening index, T is temperature, υ is a constant, $\bar{\varepsilon}$ is strain, and $\dot{\bar{\varepsilon}}$ is strain-rate.

This model has been utilized in modeling orthogonal cutting of low- and medium-carbon steels in conjunction with slip-line field analysis as an analytical solution to predict cutting forces, average strain, strain-rate, and temperatures in the primary shear zone.

Another unique flow stress model developed for metal cutting is proposed by Maekawa et al. [6] by considering the coupling effect of strain rate and temperature as well as the loading history effects of strain and temperature as

$$\bar{\sigma} = A(10^{-3}\,\dot{\bar{\varepsilon}})^M e^{kT}(10^{-3}\,\dot{\bar{\varepsilon}})^{kT} \times \left[\int_{T,\bar{\varepsilon}\equiv(\dot{\bar{\varepsilon}})} e^{-kT/N}(10^{-3}\,\dot{\bar{\varepsilon}})^{-m/N} d\bar{\varepsilon}\right]^N, \tag{3}$$

where k, m are constants and A, M, N are functions of temperature. This model also captures the blue brittleness behavior of low-carbon steels where flow stress increases with the temperature at certain deformation conditions contrary to the thermal softening behavior. The integral term accounts for the history effects of strain and temperature in relation to strain-rate. In that respect, the model is considered unique to recover history effects of strain and temperature during metal cutting. The drawback of this model is the difficulty of applying the model in finite element analysis software without modifications. Özel and Altan [3] used this empirical model in finite element modeling of high-speed cutting of annealed mold steel by linearizing the integral term.

Among many other material constitutive models, Johnson–Cook (JC) [9] and Zerilli–Armstrong (ZA) [10] models are widely used for high-strain rate applications in which models describe the flow stress of a material as functions of strain, strain rate, and temperature effects. This paper will only be concerned with those models to explore the applicability of evolutionary computation in determining model parameters for high-strain rate metal cutting regimes.

2.1. JC Model

In the JC constitutive model as given in Eq. (4), describes the flow stress as the product of strain, strain rate, and temperature effects; i.e., work hardening, strain-rate hardening, and thermal softening.

$$\bar{\sigma} = \left[A + B(\bar{\varepsilon})^n\right]\left[1 + C\ln\left(\frac{\dot{\bar{\varepsilon}}}{\dot{\bar{\varepsilon}}_0}\right)\right]\left[1 - \left(\frac{T - T_0}{T_m - T_0}\right)^m\right] \tag{4}$$

In Eq. (4) the parameter A is the initial yield strength of the material at room temperature. The equivalent plastic strain rate $\dot{\bar{\varepsilon}}$ is normalized with a reference strain rate $\dot{\bar{\varepsilon}}_0$. T_0 is room temperature, and T_m is the melting temperature of the material, and they are constants. While the parameter n takes into account the strain hardening effect, the parameter m models the thermal softening effect, and C represents strain rate sensitivity. The JC model is a well-accepted and numerically robust constitutive material model and highly utilized in modeling and simulation studies. The JC model assumes that the slope of the flow stress curve is independently affected by strain hardening, strain rate sensitivity, and thermal softening behaviors. Each of these sets is represented by the brackets in the constitutive equation.

Various researchers have conducted split Hopkinson pressure bar (SHPB) high-speed compression tests (some data is given in Fig. 1) to obtain the parameters A, B, C, n, and m of the constitutive equation by fitting the experimental data as given in Table 1. Jaspers and Dautzenberg [11] conducted SHPB compression tests for AISI 1045 steel and AA 6082-T6 and identified the JC constitutive model parameters of those materials. Lee and Lin [12] have conducted SHPB tests to investigate the high-temperature deformation behavior of Ti6Al4V, and they have found that the temperature mostly influences the flow behavior of the material. They determined JC parameters by using regression analysis and claimed that flow stress values calculated from the JC model agree well with those from the SHPB tests. Gray et al. [13] conducted high compression tests and determined constants for JC by using a computer program which performed an optimization routine to fit the experimental data. They have also used a parameter indicating the degree of fit defined by

$$\delta = \frac{1}{n}\sum_{i=1}^{n}\frac{|\sigma_{\text{calculated}}(\varepsilon_i) - \sigma_{\text{experimental}}(\varepsilon_i)|}{\sigma_{\text{experimental}}(\varepsilon_i)}. \tag{5}$$

2.2. ZA Model

Zerilli and Armstrong [10] developed a constitutive model based on dislocation-mechanics theory and considering crystal structure of materials. The model makes a distinction between body cubic centered (BCC) and face cubic centered (FCC) lattice structure of the materials as given in Eqs. (6) and (7), respectively:

$$\bar{\sigma} = C_0 + C_1\exp(-C_3T + C_4T\ln(\dot{\bar{\varepsilon}})) + C_5(\bar{\varepsilon})^n \quad \text{(BCC)} \tag{6}$$

$$\bar{\sigma} = C_0 + C_2(\bar{\varepsilon})^n\exp(-C_3T + C_4T\ln(\dot{\bar{\varepsilon}})) \quad \text{(FCC)}. \tag{7}$$

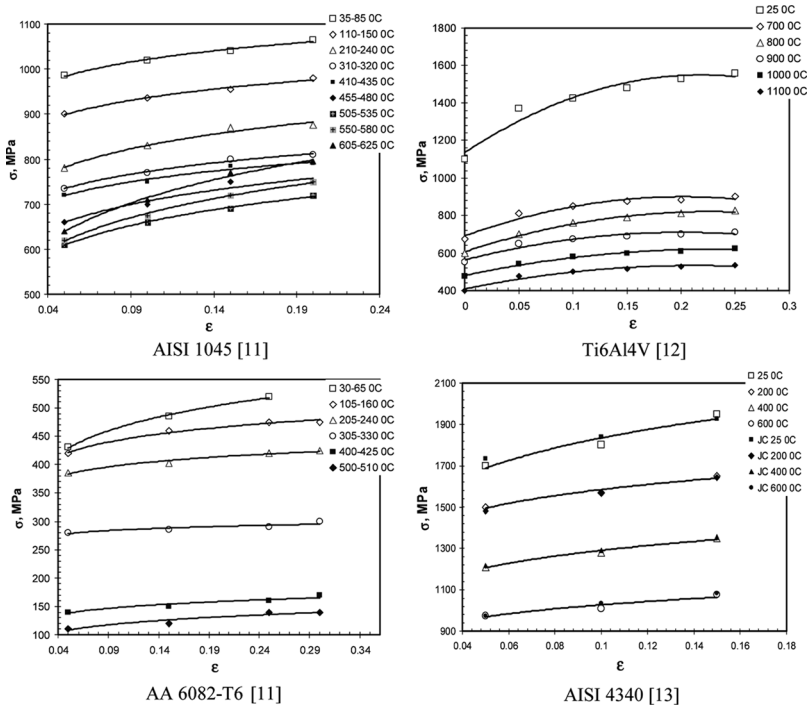

FIGURE 1.—Split-Hopkinson Pressure Bar (SHPB) compression test data.

TABLE 1.—Constants for the Johnson-Cook constitutive model*.

	AISI 1045 steel [11]	AISI 4340 steel [13]	AA 6082-T6 aluminum [11]	Ti6Al4V titanium [12]	Ti6Al4V titanium [14]
A [MPa]	553.1	2100	428.5	782.7	896
B [MPa]	600.8	1750	327.7	498.4	656
C	0.0134	0.0028	0.00747	0.028	0.0128
n	0.234	0.65	1.008	0.28	0.50
m	1	0.75	1.31	1.0	0.8
T_m [K]	1733	1783	855	1933	1933

*Reference strain-rates are 7500 s^{-1} for AISI 1045 and 10500 s^{-1} AA 6082-T6 [11], 2000 s^{-1} for Ti6Al4V [12].

In those constitutive equations C_0, C_1, C_2, C_3, C_4, C_5, and n are empirical material constants and often determined through experience based methods rather than using computational methods. For instance, Jaspers and Dautzenberg [11] have concluded that strain rate and temperature dramatically influence the flow stress of metals as they have investigated high strain rate deformation behavior of AISI 1045 steel and AA 6082-T6 aluminum with SHPB tests. Firstly, they used JC and Zerilli–Armstrong (ZA) constitutive models to identify the constants in these equations, and then compared results to the measurements. To calculate material parameters, they did not prefer to use a least square estimator method because of its difficulty. Instead the parameters are investigated by leaving only one parameter unconstrained, whereas the others are kept constant, and consequently all parameters are calculated for both models.

Meyer and Kleponis [14] also obtained constants for both JC and ZA models by using the SHPB experimental data, and then, used and compared those models in simulations of ballistic impact (a high-strain rate phenomenon) experiments for Ti6Al4V. For JC constants, they kept the constant A at the value of 896 MPa, and consequently, applied a least-square technique to find the other parameters. For the ZA model, they used a computer program to determine parameters of for the FCC constitutive equation, C_0, C_1, C_3, and C_4. The remaining parameters C_5 and n are assumed having the values of constants B and n from the JC model fitting process. For four different materials, ZA model constants are given in Table 2. Meyer and Kleponis concluded that the ZA model with the calculated constants well represented the ballistic impact with velocities up to 2000 m/s.

TABLE 2.—Constants for the ZA constitutive model*.

	AISI 1045 steel (b.c.c) [11]	AISI 4340 steel (b.c.c) [13]	AA 6082-T6 aluminum (f.c.c) [11]	Ti6Al4V (f.c.c) [14]
C_0 [MPa]	159.2	89.8	0	740
C_1 [MPa]	1533.7	2073.6	–	–
C_2 [MPa]	–	–	3551.4	240
C_3 [1/K]	0.00609	0.0015	0.00341	0.00240
C_4 [1/K]	0.000189	0.0000485	0.000057	0.000430
C_5 [MPa]	742.6	1029.4	–	656
n	0.171	0.531	–	0.5

*Reference strain-rates are 7500 s^{-1} for AISI 1045 and 10500 s^{-1} AA 6082-T6 [11], 1500, 2000, 2500 s^{-1} for AISI 4340 [13], 0.0001, 0.1, 2150 s^{-1} for Ti6Al4V [14].

3. Determination of plastic flow stress at high-strain rate conditions

Özel and Zeren [15] proposed a methodology to expand the applicability of the JC constitutive material model to the high-speed cutting regimes by utilizing orthogonal cutting tests. This methodology uses the modified parallel-sided shear zone metal cutting theory of Oxley [1] and makes use of mechanical and thermal material properties, measured forces and cut chip thicknesses obtained from orthogonal cutting tests to calculate equivalent flow stress, strain, strain rate, and temperature conditions. This methodology predicts flow stress as a function of strain, strain rate, and temperature at extended ranges, combines with the SHPB compression test data and hence widens the applicability of the JC work material model beyond the typical ranges of compression tests. A flow chart describing the methodology is given Fig. 2. The methodology can also be utilized to determine JC material constants from SHPB data only.

Identifying the JC constitutive model parameters, A, B, n, C, and m can be considered as a minimization optimization problem in the form

$$\min(\delta) = \sum_{i=1}^{k} \sqrt{\left(\bar{\sigma}^2_{\text{combined}_i} - \bar{\sigma}^2_{\text{calculated}_i}\right)} \tag{8}$$

where the $\bar{\sigma}_{\text{combined}}$ is a combined data set (measured flow stress through SHPB compression tests + predicted flow stress from orthogonal cutting tests), the $\bar{\sigma}_{\text{calculated}}$ is the calculated flow stress through the JC constitutive equation with the estimate parameters (A, B, n, C, m) and k is the total number of data points in the combined data set.

The objective of the optimization problem is to identify the JC parameters that minimize the error given in Eq. (8). For this purpose, various evolutionary computational algorithms were employed. This methodology is applied to determine constitutive models for, AISI 1045, and AISI 4340 steels, AA6082-T6 aluminum, and Ti6Al4V titanium.

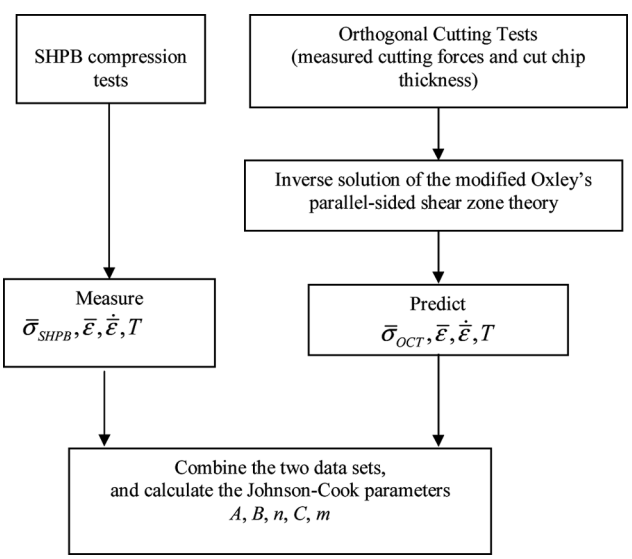

Figure 2.—Methodology to determine flow stress and obtain the parameters of the JC constitutive model.

4. Evalutionary computational algorithms

In this paper, evolutionary computational algorithms such as particle swarm optimization (PSO) and cooperative swarm intelligence (CSI) are used. Particle swarm optimization (PSO), developed by Eberhart and Kennedy [16], is a stochastic, population based optimization technique, which has been applied to solve many problems successfully. Since the idea of PSO is simple and easy to implement, it has attracted many researchers and many variations of PSO have been proposed. CSI is in fact a variation of PSO called cooperative particle swarm optimization (CPSO) as first proposed by Van der Bergh and Engelbrecht [17]. These algorithms are utilized in optimizing Eq. (6). The related influence factors (strain hardening, strain rate sensitivity, and thermal softening) are grouped together in each of the three brackets in the JC constitutive equation. A modification of the CPSO, called the CPSO-S_5, is constructed by dedicating five swarms to search for A, B, C, n, and m, each searching for one JC parameter. In the CPSO-S_5 the index S_5 indicates five swarms exist. The scheme is especially suitable to identify the parameters of the JC constitutive equation by considering five independent material parameters. It is seen that CPSO enables a more fine-grained search then PSO and yielded better results for the optimization problem studied in this paper.

PSO is initialized with a population of random solutions and this initial population evolves over generations to find optima. However, in PSO, each particle in population has a velocity, which enables them to fly through the problem space instead of dying and mutation mechanisms of genetic algorithms. Therefore, each particle is represented by a position and a velocity. Modification of the position of a particle is performed by using its previous position information and its current velocity. Each particle knows its best position (personal best) so far and the best position achieved in the group (group best) among all personal bests. These principles can be formulated as:

$$v_i^{k+1} = wv_i^k + c_1 rand_1\left(pbest_i - x_i^k\right) + c_2 rand_2(gbest - x_i^k) \tag{9}$$

where

v_i^k : velocity of agent i at iteration k

x_i^k : current position of agent i at iteration k

$pbest_i$: personal best of agent i

$gbest$: best position in group

$rand$: random number between 0 and 1

w : weighting function

c_j : weigthing factor $j = 1, 2$

$$x_i^{k+1} = x_i^k + v_i^{k+1} \tag{10}$$

The first term on the right-hand side of Eq. (9) is the previous velocity of the particle, which enables it to fly in search space. The second and third terms are used to change the velocity of the agent according to *pbest* and *gbest*. This concept is similar to the human decision process where a person makes his/her decision using his own experiences and other people's experiences.

The flow chart of the PSO algorithm is given in Fig. 3. The iterative approach of PSO can be described as follows:

1. Initial position and velocities of the agent are generated. The current position of each particle is set as *pbest*. The *pbest* with best value is set as *gbest* and this value is stored. The next position is evaluated for each particle by using Eqs. (9) and (10).

2. The objective function value is calculated for new positions of each particle. If a better position is achieved by an agent, the *pbest* value is replaced by the current value. As in Step 1, a *gbest* value is selected among *pbest* values. If the new *gbest* value is better than the previous *gbest* value, the *gbest* value is replaced by the current *gbest* value and stored.

3. Steps 1 and 2 are repeated until the iteration number reaches a predetermined iteration number.

PSO's success depends on the selection of parameters given in Eq. (9). Shi and Eberhardt [18] studied the effects of parameters and concluded that c_1 and c_2 can be taken around the value of 2 independent of the problem. Inertia weight w is usually utilized according to the formula

$$w = w_{\max} - \frac{w_{\max} - w_{\min}}{iter_{\max}} \times iter \tag{11}$$

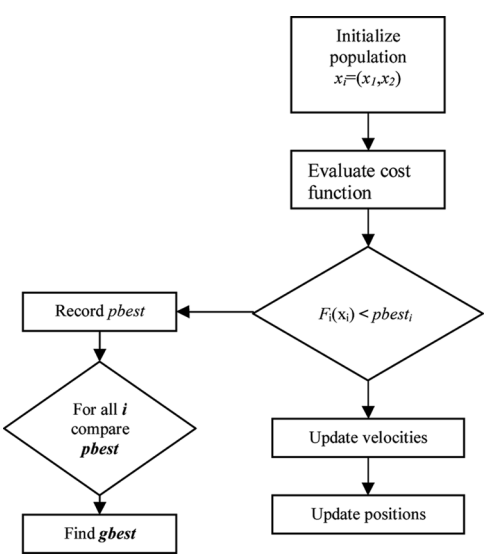

FIGURE 3.—Flowchart of PSO algorithm.

where

$w_{\max}$: initial weight
$w_{\min}$: final weight
$iter_{\max}$: maximum iteration number
$iter$: current iteration number

Equation (11) decreases the effect of velocity towards the end of the search algorithm, which confines the search in a small area to find optima accurately. Clerc [19] proposed the use of a constriction factor to insure convergence of the particle swarm algorithm and modified the velocity calculation as in Eq. (12). The basic equations of PSO were considered as difference equations and investigated by eigenvalue analysis which controls the behavior of the system. Eberhart and Shi [20] verified the effectiveness of the constriction factor approach.

$$v_i^{k+1} = K \cdot \left(v_i^k + c_1 rand_1 (pbest_i - x_i^k) + c_2 rand_2 (gbest - x_i^k)\right) \tag{12}$$

where

$$K = \frac{2}{\left|2 - \varphi - \sqrt{\varphi^2 - 4.\varphi}\right|}$$
$$\varphi = c_1 + c_2$$
$$\varphi > 4$$

The velocity update step in PSO is stochastic due to random numbers generated, which may cause an uncontrolled increase in velocity and therefore instability in search algorithm. In order to prevent this, usually a maximum and a minimum allowable velocity are selected and implemented in the algorithm. In practice, these velocities are selected depending on the parameters of the problem or, as proposed in Eberhart and Shi [20], can be limited to the dynamic range of maximum position variable on each dimension.

The original PSO is developed to solve continuous optimization problems. However, engineering problems may have discrete variables. Kennedy and Eberhart [21] developed a discrete binary version of PSO. In this version velocity corresponding to the discrete dimension of a particle is considered as probability of position being in one state or in another depending on the value of velocity. If velocity is high, the particle is more likely to choose "1" and low values will indicate a "0" choice. This can be accomplished by constraining the velocity term in interval [0, 1] by a sigmoid function. The necessary modifications in the general formula of PSO are:

$$v_i^{k+1} = K\left(v_i^k + c_1 rand_1 (pbest_i - x_i^k) + c_2 rand_2 (gbest - x_i^k)\right)$$

$$sig(v_i^{k+1}) = \frac{1}{1 + \exp(-v_i^{k+1})}$$

$$x_i^{k+1} = \begin{Bmatrix} 0 \; sig\left(v_i^{k+1}\right) \le \rho \\ 1 \; sig\left(v_i^{k+1}\right) > \rho \end{Bmatrix}$$

$$\rho = \text{random number between } [0, 1].$$

Angeline [22] introduced a natural selection mechanism which is utilized in all evolutionary computation algorithms in PSO by replacing poor performing particles with good performing particles over the iterations. Therefore the number of lowly evaluated poor performing agents decreased at each iteration. This method is called *hybrid PSO* (HPSO). It helps PSO converge much faster and ensures a search in a more concentrated area.

The above given computational algorithms are used in Matlab® programs as three consecutive methods: (i) classical particle swarm optimization (PSO), (ii) particle swarm optimization with a constriction factor approach (PSO-c), and (iii) cooperative particle swarm optimization where each swarm finds individual constants of the constitutive equation (CPSO). These Matlab® programs are integrated with the flow stress determination computer programs to identify the unknown constants of the constitutive equations such as JC and ZA.

5. Results and discussion

Proposed flow stress determination methodology using evolutionary computational methods of PSO, PSO-c, and CSPO is utilized to identify the JC, constants for AISI 1045 steel, AISI 4340 steel, AA6082 aluminum, and Ti6Al4V titanium alloy by using SHPB test data generated by Jaspers and Dautzenberg [11], Gray et al. [13], and Meyer et al. [14], respectively. The identified constants are given in Tables 3–6. For those materials, a comparison for the measured flow stress at various temperatures and strain with respect to flow stress data generated using the JC constitutive equation with identified constants using evolutionary algorithms is provided in Figs. 4–7. It can be seen from these figures that the evolutionary computational approach, especially CPSO, outperformed the solutions provided by the owners of the data for AISI 1045 steel, AISI 4340 steel, and AA 6082 aluminum with the exception of Ti6Al4V. In the case of Ti6Al4V, flow stress computed using CPSO fitted to the JC model has come close to the predicted flow stress originally proposed by Lee and Lin [12]. It can be seen that CPSO provided a more fine-grained search then PSO in almost all cases and yielded better results in optimizing parameters of the JC material model for the best fit.

Table 3.—Identified JC constitutive model constants for AISI 1045 steel.

AISI 1045 steel	Jaspers–Dautzenberg solution [11]	PSO	PSO-c	CPSO
A [MPa]	553.1	646.19	731.63	546.83
B [MPa]	600.8	517.7	518.7	609.35
C	0.0134	0.0102	0.00571	0.01376
n	0.234	0.24597	0.3241	0.2127
m	1	0.94054	0.94054	0.94053

Table 4.—Identified JC constitutive model constants for AISI 4340 steel.

AISI 4340 steel	Gray et al. solution [13]	PSO	CPSO
A [MPa]	2100	1547.3	1523.3
B [MPa]	1750	1638.4	1022.6
C	0.0028	0.00005	0.001512
n	0.65	0.75	0.5358
m	0.75	0.9016	0.89438

Table 5.—Identified JC constitutive model constants for Ti6Al4V steel.

Ti6Al4V titanium	Lee and Lin solution [12]	PSO	PSO-c	CPSO
A [MPa]	782.7	803.85	883.99	987.8
B [MPa]	498.4	544.57	598.87	761.5
C	0.028	0.05	0.0335	0.01516
n	0.28	0.36166	0.36166	0.41433
m	1	1.041	1.041	1.516

Table 6.—Identified JC constitutive model constants for AA6082.

AA 6082 aluminum	Jaspers–Dautzenberg solution [11]	PSO	CPSO
A [MPa]	428.5	400.5	403.57
B [MPa]	327.7	285.17	306.56
C	0.00747	0.0004	0.00185
n	1.008	0.6607	0.7769
m	1.31	1.3494	1.73

Conclusion

This work presents a micromechanical approach to study deformation behavior of work materials in high-strain rate metal cutting conditions and utilizes evolutionary computational methods. The JC constitutive model and cooperative particle swarm optimization (CPSO) are combined to investigate the effects of high-strain rate dependency, thermal softening, and strain rate-temperature coupling on the material flow stress. The methodology is applied in predicting JC constitutive model parameters, and the results are compared with the other solutions. Evolutionary computational algorithms have outperformed the classical data fitting solutions. This methodology can also be extended to other constitutive material models. The following conclusions can be made:

(1) Work material constitutive models can be highly deficient to represent the plasticity behavior of the materials at elevated temperatures and high strain rates.
(2) Fitting experimentally obtained flow stress at various strain, strain-rate, and temperature to a simple elegant

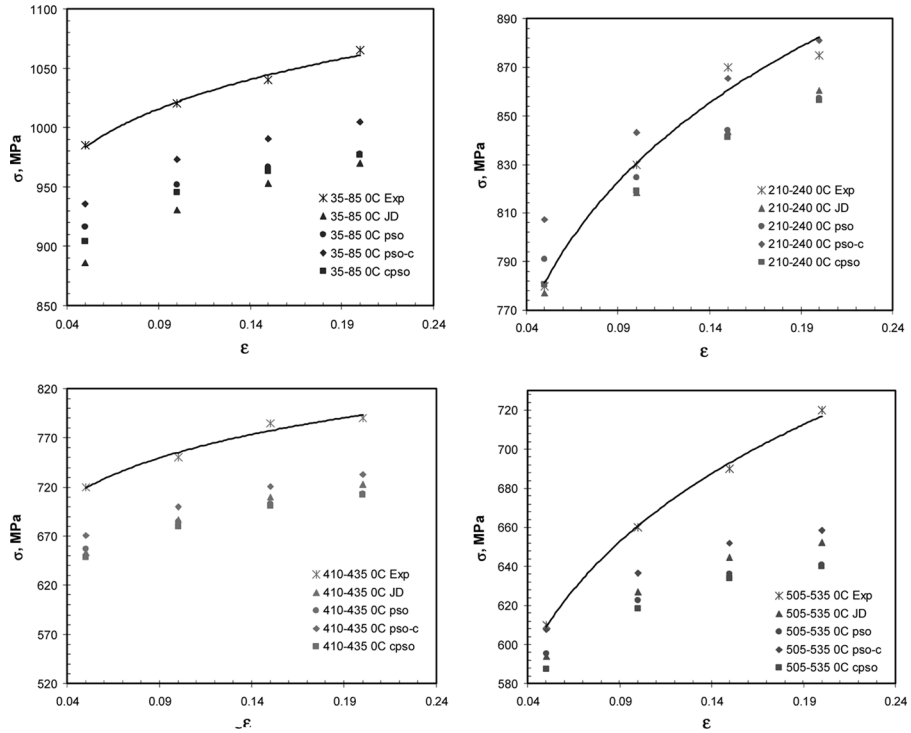

FIGURE 4.—Comparison of experimental flow stress data with data generated from the fitted constitutive equation (AISI 1045).

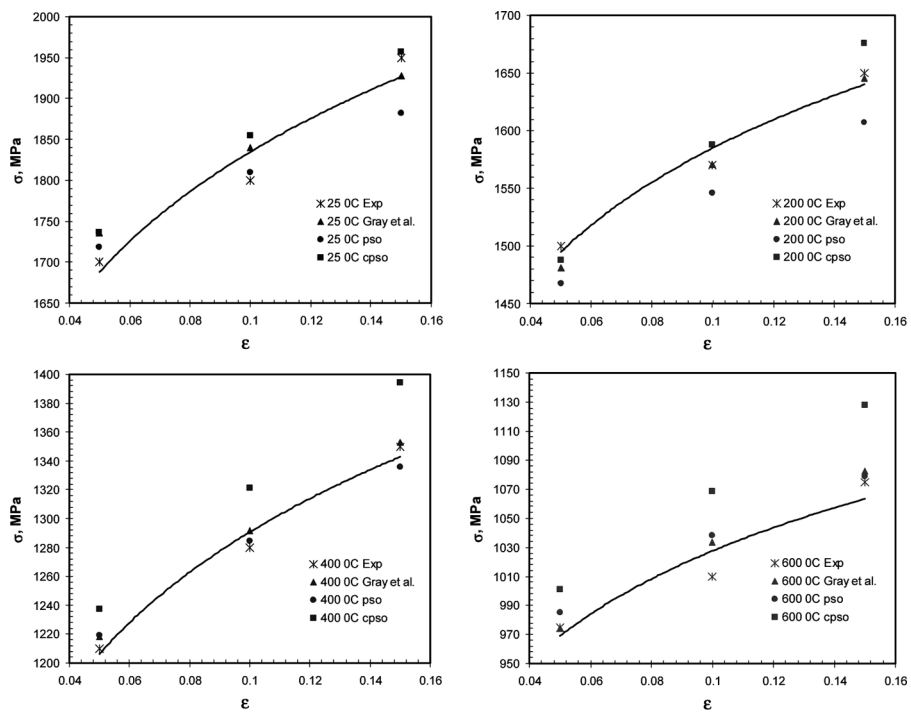

FIGURE 5.—Comparison of experimental flow stress data with data generated from the fitted constitutive equation (AISI 4340).

constitutive model is an important effort and must be performed using advanced computational methods.

(3) Evolutionary computational methods such as particle swarm optimization and cooperative particle swarm optimization have been proven to be highly effective in determining the constants and parameters of the constitutive material models.

(4) It is seen that CPSO enables a more fine-grained search then PSO and yielded better results for the optimization problem studied in this paper.

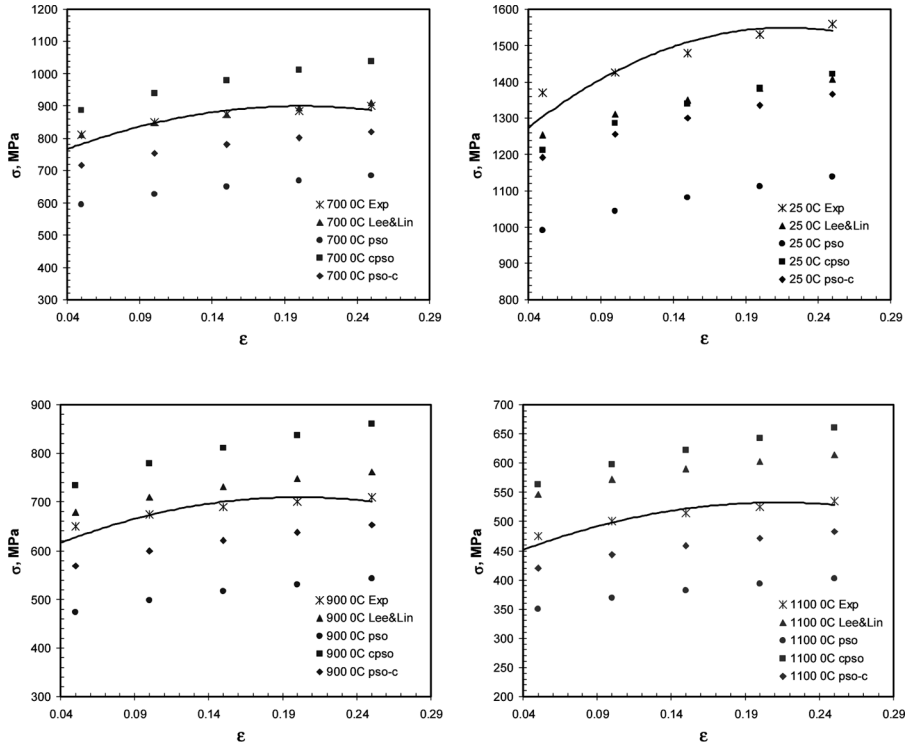

FIGURE 6.—Comparison of experimental flow stress data with data generated from the fitted constitutive equation (Ti6Al4V).

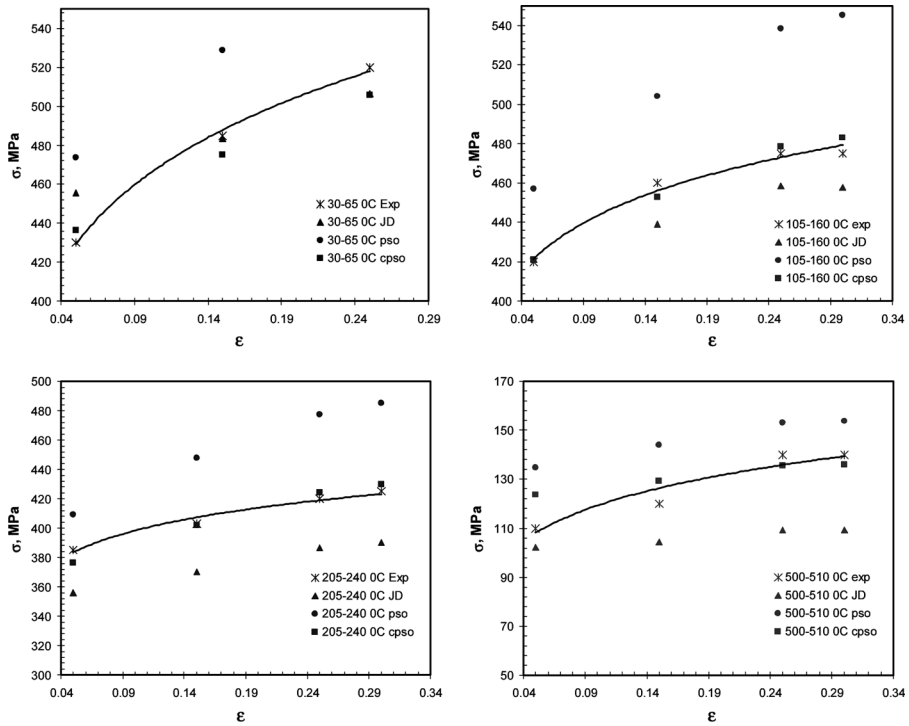

FIGURE 7.—Comparison of experimental flow stress data with data generated from the fitted constitutive equation (AA 6082-T6).

References

1. Oxley, P.L.B. *Mechanics of Machining, An Analytical Approach to Assessing Machinability*; Ellis Horwood Limited: Chichester, UK, 1989.
2. Childs, T.H.C.; Maekawa, K.; Obikawa, T.; Yamane, Y. *Metal Machining: Theory and Applications*; Arnold: London, U.K., 2000.
3. Özel, T.; Altan, T. Determination of workpiece flow stress and friction at the chi-tool contact for high speed cutting. International Journal of Machine Tool and Manufacture **2000**, *40*, 1333–1352.
4. Sartkulvanich, P.; Altan, T.; Abdullah, G. Effects of flow stress and friction models in finite element simulation of orthogonal cutting—a sensitivity analysis. Machining Science and Technology **2005**, *9*, 1–26.
5. Jaspers, S.P.F.C.; Dautzenberg, J.H. Material behaviour in metal cutting: strains, strain rates and temperatures in chip formation. Journal of Materials Processing Technology **2002**, *121*, 123–135.
6. Maekawa, K.; Shirakashi, T.; Usui, E. Flow stress of low carbon steel at high temperature and strain rate (Part 2). Bulletin, Japanese Society of Precision Engineering **1983**, *17/3*, 167–172.
7. Bammann, D.J.; Chiesa, M.L.; Johnson, G.C. Modeling large deformation and failure in manufacturing processes. Theoretical and Applied Mechanics **1996**, 359–376.
8. Lennon, A.M.; Ramesh, K.T. A technique for measuring the dynamic behavior of materials at high temperatures. International Journal of Plasticity **1998**, *14/12*, 1279–1292.
9. Johnson, G.R.; Cook, W.H. A constitutive model and data for metals subjected to large strains, high strain rates and high temperatures. Proceedings of the 7th International Symposium on Ballistics, The Hague, The Netherlands, 1983; 541–547.
10. Zerilli, F.J.; Armstrong, R.W. Dislocation mechanics based constitutive relations for material dynamics calculations. Journal of Applied Physics **1987**, *61/5*, 1816–1825.
11. Jaspers, S.P.F.C; Dautzenberg, J.H. Material behavior in conditions similar to metal cutting: flow stress in the primary shear zone. Journal of Materials Processing Technology **2002**, *122*, 322–330.
12. Lee, W.S.; Lin, C.F. High-temperature deformation behavior of Ti6Al4V alloy evaluated by high strain-rate compression tests. Journal of Materials Processing Technology **1998**, *75*, 127–136.
13. Gray, G.T.; Chen, S.R.; Wright, W.; Lopez, M.F. Constitutive equations for annealed metals under compression at high strain rates and high temperatures. *Los Alamos National Laboratory Report*; LA-12669-MS, 1994.
14. Meyer H.W. Jr.; Kleponis, D.S. Modeling the high strain rate behavior of titanium undergoing ballistic impact and penetration. International Journal of Impact Engineering **2001**, *26*, 509–521.
15. Özel, T.; Zeren, E. A methodology to determine work material flow stress and tool-chip interfacial friction properties by using analysis of machining. ASME Journal of Manufacturing Science and Engineering **2006**, *128*, 119–129.
16. Eberhart, R.C.; Kennedy, J. Particle swarm optimization. Proceedings of IEEE International Conference on Neural Networks, Piscataway, NJ, 1995; 942–1948.
17. Van der Bergh, F.; Engelbrecht, A.P. A cooperative approach to particle swarm optimization. IEEE Transactions on Evolutionary Computation **2004**, *8* (3), 225–239.
18. Shi, Y.; Eberhart, R.C. Parameter selection in particle swarm optimization. Proceedings of 7th Annual Conference on Evalutionary Programming, San Diego, 1998; 591–600.
19. Clerc, M. The swarm and the queen: toward a deterministic and adaptive particle swarm optimization. In Proceedings of 1999 Congress on Evolutionary Computation, Washington, DC, 1999; 1951–1957.
20. Eberhart, R.C.; Shi, Y. Comparing inertia weights and constriction factors in particle swarm optimization. In Proceedings of 2000 Congress on Evolutionary Computation, La Jolla, CA, 2000; 84–88.
21. Kennedy, J.; Eberhart, R.C. A discrete binary version of the particle swarm algorithm. In Proceedings of IEEE International Conference on Systems, Man, and Cybernetics, Computational Cybernetics and Simulation, Orlando, FL, 1997; 5, 4104–4108.
22. Angeline, P. Using selection to improve particle swarm optimization. In Proceedings of 1999 Congress on Evolutionary Computation, Washington, DC, 1999; 84–89.